Organophosphine Oxide/Sulfide-Substituted Lanthanide Binaphtholate Catalysts for Enantioselective Hydroamination/Cyclization

Xianghua Yu and Tobin J. Marks*

Department of Chemistry, Northwestern University, 2145 Sheridan Road, Evanston, Illinois 60208

Received September 1, 2006

A series of chiral organophosphine oxide/sulfide-substituted binaphtholate ligands have been prepared ($\{(R)$-H_2BINOL-$[P(O)R_2]_2\}^{2-}$, R = Ph, Et, ^{t}Bu, 3,5-xylyl, Bn, and OEt; $\{(R)$-H_2BINOL-$[P(S)Ph_2]_2\}^{2-}$). The X-ray crystal structures of (R)-H_2BINOL-$[P(O)R_2]_2$ (R = Ph, Et, and ^{t}Bu) evidence the varying binaphtholate dihedral angles and conformational flexibility possible for these ligands. Precatalysts for enantioselective intramolecular aminoalkene hydroamination/cyclization are conveniently generated in situ from the metal homoleptic dialkylamido precursors $Ln[N(SiMe_3)_2]_3$ (Ln = La, Nd, Sm, Y, Lu, and Sc) and the above binaphthols. The crystal structure of $La_2\{(R)$-BINOL-$[P(O)Ph_2]_2\}_3$ reveals strong coordination of lanthanide ion by the phosphine oxide moieties. Enantioselectivities as high as 65% ee for the hydroamination/cyclization of 2,2-dimethylpent-4-enylamine are obtained with $\{(R)$-BINOL-$[P(O)Et_2]_2\}NdN(SiMe_3)_2$ at room temperature. Lanthanide catalysts having varying organophosphine oxide-substituted binaphtholate ligands exhibit differing enantioselectivity trends with decreasing Ln^{3+} ionic radius, whereas Sc^{3+} catalysts afford enantioselectivities with opposite product configurations. Kinetic studies reveal that the hydroamination rate is zero-order in [aminoalkene], consistent with the generally accepted mechanism for organolanthanide-catalyzed hydroamination/cyclization.

Introduction

Due to its marked atom economy, the intramolecular hydroamination (HA) of alkenes, alkynes, dienes, and allenes is an attractive process for the catalytic synthesis of nitrogen-containing organic compounds (eq 1).[1,2] Moreover, the nitrogen-containing heterocycles obtained via hydroamination/cyclization processes are frequently found in numerous pharmacologically active compounds. Since the initial reports from this laboratory of highly active organolanthanide complexes for intramolecular aminoalkene hydroamination,[3v] we have focused on exploring the scope and selectivity of this process.[3]

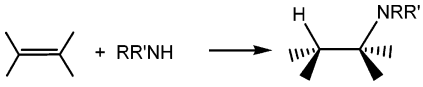

(1)

Enantioselective hydroamination using chiral lanthanide catalysts represents one of the most desirable, elegant, and challenging C−N bond-forming transformations, enabling the synthesis of chiral amines in a single step.[4−9] During the past several years, a number of lanthanide catalysts have been discovered for this purpose, and their representative structures are shown in Scheme 1. The first catalytic enantioselective intramolecular HA/cyclization of aminoalkenes reported from our group utilized C_1-symmetric *ansa*-lanthanocene catalysts (structures **A** and **B** in Scheme 1) and afforded chiral pyrro-

* Corresponding author. E-mail: t-marks@northwestern.edu.

(1) For general C−N bond formation references, see: (a) Beller, M.; Seayad, J.; Tillack, A.; Jiao, H. *Angew. Chem., Int. Ed.* **2004**, *43*, 3368−3398. (b) Beller, M.; Tillack, A.; Seayad, J. Catalytic Amination Reactions of Olefins and Alkynes. In *Transition Metals for Organic Synthesis*, 2nd ed.; Beller, M., Bolm, C., Eds.; Wiley-VCH: Weinheim, Germany, 2004; Vol. 2. (c) Hartwig, J. F. *Science* **2002**, *297*, 1653−1654. (d) Beller, M.; Riermeier, T. H. Transition Metal-catalyzed C-N and C-O Bond-forming Reactions. In *Transition Metals for Organic Synthesis*, 1st ed.; Beller, M., Bolm, C., Eds.; Wiley-VCH: Weinheim, Germany, 1998; Vol. 1. (e) Hegedus, L. S. *Angew. Chem., Int. Ed. Engl.* **1988**, *27*, 1113−1226.

(2) For general hydroamination reviews, see: (a) Odom, A. L. *Dalton Trans.* **2005**, 225−233. (b) Hong, S.; Marks, T. J. *Acc. Chem. Res.* **2004**, *37*, 673−686. (c) Doye, S. *Synlett* **2004**, 1653−1672. (d) Roesky, P. W.; Müller, T. E. *Angew. Chem., Int. Ed.* **2003**, *42*, 2708−2710. (e) Pohlki, F.; Doye, S. *Chem. Soc. Rev.* **2003**, *32*, 104−114. (f) Bytschkov, I.; Doye, S. *Eur. J. Org. Chem.* **2003**, 935−946. (g) Seayad, J.; Tillack, A.; Hartung, C. G.; Beller, M. *Adv. Synth. Catal.* **2002**, *344*, 795−813. (h) Togni, A. Hydroamination. In *Catalytic Heterofunctionalization from Hydroamination to Hydrozirconation*, 1st ed.; Togni, A., Grüetzmacher, H., Eds.; Wiley-VCH: New York, 2001; pp 91−141. (i) Nobis, M.; Driessen-Hölscher, B. *Angew. Chem., Int. Ed.* **2001**, *40*, 3983−3985. (j) Eisen, M. S.; Straub, T.; Haskel, A. *J. Alloys Comp.* **1998**, 271−273, 116−122. (k) Müller, T. E.; Beller, M. *Chem. Rev.* **1998**, *98*, 675−704.

(3) (a) Motta, A.; Lanza, G.; Fragalà, I. L.; Marks, T. J. *Organometallics* **2004**, *23*, 4097−4104. (b) Seyam, A. M.; Stubbert, B. D.; Jensen, T. R.; O'Donnell, J. J., III; Stern, C. L.; Marks, T. J. *Inorg. Chim. Acta* **2004**, *357*, 4029−4035. (c) Ryu, J.-S.; Marks, T. J.; McDonald, F. E. *J. Org. Chem.* **2004**, *69*, 1038−1052. (d) Hong, S.; Kawaoka, A. M.; Marks, T. J. *J. Am. Chem. Soc.* **2003**, *125*, 15878−15892. (e) Hong, S.; Tian, S.; Metz, M. V.; Marks, T. J. *J. Am. Chem. Soc.* **2003**, *125*, 14768−14783. (f) Ryu, J.-S.; Li, G. Y.; Marks, T. J. *J. Am. Chem. Soc.* **2003**, *125*, 12584−12605. (g) Hong, S.; Marks, T. J. *J. Am. Chem. Soc.* **2002**, *124*, 7886−7887. (h) Ryu, J.-S.; Marks, T. J.; McDonald, F. E. *Org. Lett.* **2001**, *3*, 3091−3094. (i) Arredondo, V. M.; Tian, S.; McDonald, F. E.; Marks, T. J. *J. Am. Chem. Soc.* **1999**, *121*, 3633−3639. (j) Arredondo, V. M.; McDonald, F. E.; Marks, T. J. *Organometallics* **1999**, *18*, 1949−1960. (k) Tian, S.; Arredondo, V. M.; Stern, C. L.; Marks, T. J. *Organometallics* **1999**, *18*, 2568−2570. (l) Arredondo, V. M.; McDonald, F. E.; Marks, T. J. *J. Am. Chem. Soc.* **1998**, *120*, 4871−4872. (m) Li, Y.; Marks, T. J. *J. Am. Chem. Soc.* **1998**, *120*, 1757−1771. (n) Roesky, P. W.; Stern, C. L.; Marks, T. J. *Organometallics* **1997**, *16*, 4705−4711. (o) Li, Y.; Marks, T. J. *J. Am. Chem. Soc.* **1996**, *118*, 9295−9306. (p) Li, Y.; Marks, T. J. *Organometallics* **1996**, *15*, 3770−3772. (q) Li, Y.; Marks, T. J. *J. Am. Chem. Soc.* **1996**, *118*, 707−708. (r) Giardello, M. A.; Conticello, V. P.; Brard, L.; Gagné, M. R.; Marks, T. J. *J. Am. Chem. Soc.* **1994**, *116*, 10241−10254. (s) Giardello, M. A.; Conticello, V. P.; Brard, L.; Sabat, M.; Rheingold, A. L.; Stern, C. L.; Marks, T. J. *J. Am. Chem. Soc.* **1994**, *116*, 10212−10240. (t) Li, Y.; Fu, P.-F.; Marks, T. J. *Organometallics* **1994**, *13*, 439−440. (u) Gagné, M. R.; Brard, L.; Conticello, V. P.; Giardello, M. A.; Stern, C. L.; Marks, T. J. *J. Am. Chem. Soc.* **1992**, *11*, 2003−2005. (v) Gagné, M. R.; Stern, C. L.; Marks, T. J. *J. Am. Chem. Soc.* **1992**, *114*, 275−294. (w) Gagné, M. R.; Marks, T. J. *J. Am. Chem. Soc.* **1989**, *111*, 4108−4109.

10.1021/om0607999 CCC: $37.00
Publication on Web 12/14/2006

Scheme 1. Representative Chiral Lanthanide Catalysts for Enantioselective Hydroamination/Cyclization

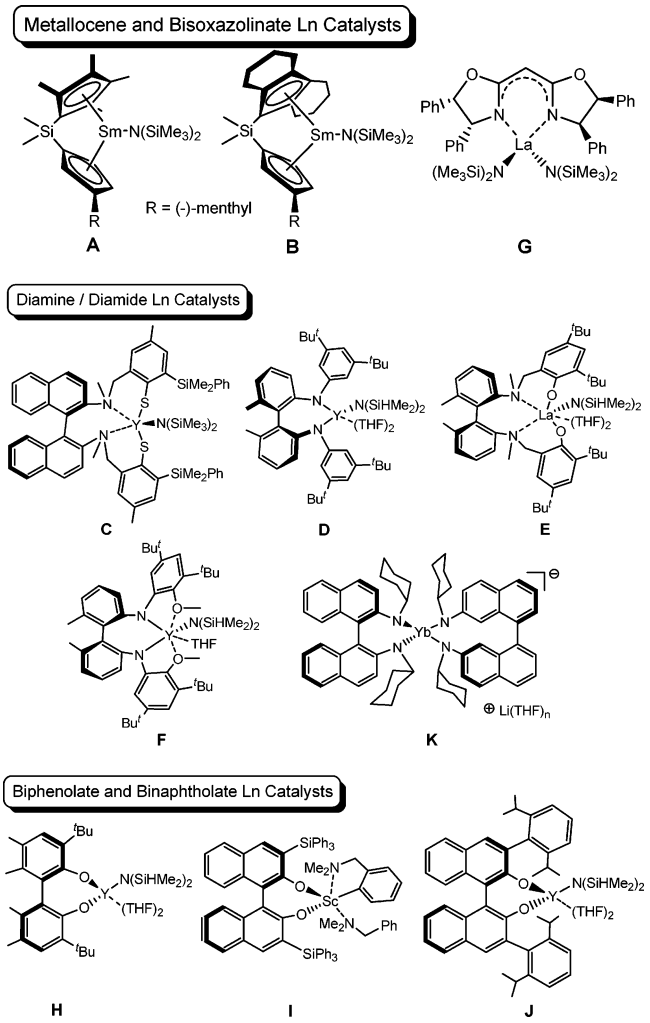

lidines in up to 74% ee.[3u] However, this application using *ansa*-lanthanocene complexes substituted by a chiral menthyl or neomenthyl group was constrained by a facile catalyst epimerization process involving reversible protonolysis of the −CpR* ligand.[3s] Results of this nature prompted several laboratories to pursue Cp-free catalyst ligands that with chirality-locked architectures would retain their configuration during the HA process.

Livinghouse and co-workers described the activity of Ln-$[N(SiMe_3)_2]_3$ for the HA/cyclization of aminopentenes to racemic pyrrolidines.[6] This work led to the synthesis of nonmetallocene lanthanide complexes as catalysts for intramolecular aminoalkene HA/cyclization. An 87% enantioselectivity for HA/cyclization was reported several years later using yttrium bisthiophenolate catalysts prepared in situ from a homoleptic yttrium amide and a bisthiolate ligand derived from binaphthyl diamine (**C**).[6a] Scott et al. subsequently reported chiral bisarylamide (such as **D**) and bisaryloxide lanthanide complexes (such as **E** and **F**) prepared from salicylaldimine-type ligands and which catalyze aminoalkene HA/cyclization reactions at 100 °C with enantiomeric excesses as high as 61% with catalyst **E**.[7] Furthermore, a chiral zirconium alkyl cation coordinated by a similar aminobiphenoxide ligand proved to be competent for the enantioselective hydroamination/cyclization of secondary aminoalkenes (up to 82% ee).[7a] Using a series of C_2-symmetric lanthanide bisoxazolinates, a broad family of enantioselective catalysts was also prepared and shown to be active at room temperature for exploratory cyclizations (up to 67% ee with **G**).[3e] Hultzsch et al. synthesized various sterically hindered rare earth metal biphenolates and binaphtholates (**H**, **I**, and **J**).[8] The scandium 3,3′-tris(phenylsilyl)binaphtholate complex (**I**) proved to be a highly active catalyst for intramolecular hydroamination and catalyzed aminopentene cyclization in 95% ee.[8a] Collin's group also reported that lanthanide *ate*-complexes derived from chiral disubstituted (*R*)-binaphthylamido ligands (**K**) afford a maximum HA/cyclization selectivity of 78% ee.[9] Even though 95% ee has been achieved for a single substrate, enantioselective hydroamination still presents a great many challenges, such as finding catalytic systems that exhibit broad selectivity and useful turnover frequencies over many substrate classes.

Organophosphine oxide- and sulfide-substituted binaphtholates $\{BINOL\text{-}[P(O)R_2]_2\}^{2-}$ and $\{BINOL\text{-}[P(S)R_2]_2\}^{2-}$ are potentially attractive ligands for enantioselective transformations catalyzed by large lanthanide ions because of two factors: (1) The dimensions and configurational stability of the binaphtholate ligands and (2) an available array of stereodirecting hard donor coordination sites that should strongly bind lanthanide ions (Scheme 2). Binaphtholate ligands are well-known for their stable chirality at high temperatures.[10] Phosphine oxide ligands are among the most commonly used, strongly binding auxiliary

(4) For additional examples of group 3- and lanthanide-catalyzed hydroamination, see: (a) Meyer, N.; Zulys, A.; Roesky, P. W. *Organometallics* **2006**, *25*, 4179−4182. (b) Bambirra, S.; Meetsma, A.; Hessen, B. *Organometallics* **2006**, *25*, 3454−3462. (c) Panda, T. K.; Zulys, A.; Gamer, M. T.; Roesky, P. W. *Organometallics* **2005**, *24*, 2197−2202. (d) Kim, J. Y.; Livinghouse, T. *Org. Lett.* **2005**, *7*, 4391−4393. (e) Molander, G. A.; Hasegawa, H. *Heterocycles* **2004**, *64*, 467−474. (f) Lauterwasser, F.; Hayes, P. G.; Bräse, S.; Piers, W. E.; Schafer, L. L. *Organometallics* **2004**, *23*, 2234−2237. (g) Hultzsch, K. C.; Hampel, F.; Wagner, T. *Organometallics* **2004**, *23*, 2601−2612. (h) Kim, Y. K.; Livinghouse, T.; Horino, Y. *J. Am. Chem. Soc.* **2003**, *125*, 9560−9561. (i) Molander, G. A.; Pack, S. K. *Tetrahedron* **2003**, *59*, 10581−10591. (j) Molander, G. A.; Pack, S. K. *J. Org. Chem.* **2003**, *68*, 9214−9220. (k) Bürgstein, M. R.; Berberich, H.; Roesky, P. W. *Chem.−Eur. J.* **2001**, *7*, 3078−3085. (l) Molander, G. A.; Dowdy, E. D. *J. Org. Chem.* **1999**, *64*, 6515−6517. (m) Molander, G. A.; Dowdy, E. D. *J. Org. Chem.* **1998**, *63*, 8983−8988.

(5) For reviews of enantioselective catalysis with lanthanides, see: (a) Hultzsch, K. C.; Gribkov, D. V.; Hampel, F. *J. Organomet. Chem.* **2005**, *690*, 4441−4452. (b) Hultzsch, K. C. *Org. Biomol. Chem.* **2005**, *3*, 1819−1824. (c) Hultzsch, K. C. *Adv. Synth. Catal.* **2005**, *347*, 367−391. (d) Aspinall, H. C. *Chem. Rev.* **2002**, *102*, 1807−1850. (e) Inanaga, J.; Furuno, H.; Hayano, T. *Chem. Rev.* **2002**, *102*, 2211−2225. (f) Molander, G. A. *Pure Appl. Chem.* **2000**, *72*, 1757−1761.

(6) (a) Kim, J. Y.; Livinghouse, T. *Org. Lett.* **2005**, *7*, 1737−1739. (b) Kim, Y. K.; Livinghouse, T. *Angew. Chem., Int. Ed.* **2002**, *41*, 3645−3647. (c) Kim, Y. K.; Livinghouse, T.; Bercaw, J. E. *Tetrahedron Lett.* **2001**, *42*, 2933−2935.

(7) (a) Knight, P. D.; Munslow, I.; O'Shaughnessy, P. N.; Scott, P. *Chem. Commun.* **2004**, 894−895. (b) O'Shaughnessy, P. N.; Gillespie, K. M.; Knight, P. D.; Munslow, I. J.; Scott, P. *Dalton Trans.* **2004**, 2251−2256. (c) O'Shaughnessy, P. N.; Scott, P. *Tetrahedron Asymmetry* **2003**, *14*, 1979−1983. (d) O'Shaughnessy, P. N.; Knight, P. D.; Morton, C.; Gillespie, K. M.; Scott, P. *Chem. Commun.* **2003**, 1770−1771.

(8) (a) Gribkov, D. V.; Hultzsch, K. C.; Hampel, F. *J. Am. Chem. Soc.* **2006**, *128*, 3748−3759. (b) Gribkov, D. V.; Hultzsch, K. C. *Chem. Commun.* **2004**, 730−731. (c) Gribkov, D. V.; Hampel, F.; Hultzsch, K. C. *Eur. J. Inorg. Chem.* **2004**, 4091−4101. (d) Gribkov, D. V.; Hultzsch, K. C.; Hampel, F. *Chem.−Eur. J.* **2003**, *9*, 4796−4810.

(9) (a) Riegert, D.; Collin, J.; Meddour, A.; Schulz, E.; Trifonov, A. *J. Org. Chem.* **2006**, *71*, 2514−2517. (b) Collin, J.; Daran, J.-C.; Jacquet, O.; Schulz, E.; Trifonov, A. *Chem.−Eur. J.* **2005**, *11*, 3455−3462. (c) Collin, J.; Daran, J. C.; Schulz, E.; Trifonov, A. *Chem. Commun.* **2003**, 3048−3049.

(10) (a) Brunel, J. M. *Chem. Rev.* **2005**, *105*, 857−897. (b) Meca, L.; Řeha, D.; Havlas, Z. *J. Org. Chem.* **2003**, *68*, 5677−5680.

Scheme 2. Organophosphine Oxide- and Sulfide-Substituted Binaphtholate Ligands Investigated

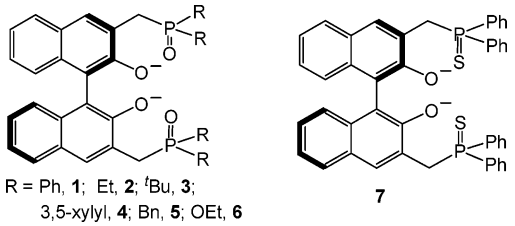

ligands for typically "hard", Lewis acidic lanthanide ions.[11] Organophosphine oxide-substituted binaphtholate ligands were first employed by Shibasaki's group in bifunctional aluminum catalysts for several transformations, such as Reissert-type insertions.[12] Here the bound Al^{3+} ion functions as a Lewis acid to activate the substrate carbonyl group, while the phosphine oxide oxygen atom functions as a Lewis base to activate silylated nucleophiles. Organophosphine-substituted binaphtholate ligands with phosphine sulfide moieties are somewhat "softer" Lewis bases and generally bind more weakly to the corresponding lanthanide ions.[13] These characteristics should provide an informative comparison.

Herein, we report the synthesis of a series of chiral organophosphine oxide/sulfide-substituted binaphtholate ligands ($\{(R)$-BINOL-$[P(O)R_2]_2\}^{2-}$ and $\{(R)$-BINOL-$[P(S)R_2]_2\}^{2-}$, Scheme 2), the synthesis and characterization of their lanthanide complexes, and their competence for enantioselective hydroamination/cyclization catalysis. The crystallographic characterization of several of the neutral ligand precursors and that of the lanthanide complex $La_2\{(R)$-BINOL-$[P(O)Ph_2]_2\}_3$ are also presented. It will be seen that these organophosphine oxide-substituted binaphtholate ligands bind strongly to lanthanide ions and that the resulting catalysts show modest to good enantioselectivities for a variety of aminoalkene HA/cyclization conversions.

Experimental Section

Materials and Methods. All manipulations of air-sensitive materials were carried out with rigorous exclusion of oxygen and moisture in flame- or oven-dried Schlenk-type glassware on a dual-manifold Schlenk line, interfaced to a high-vacuum line (10^{-6} Torr), or in a nitrogen-filled Vacuum Atmospheres glovebox with a high-capacity recirculator (<1 ppm of O_2). Argon (Airgas, prepurified) was purified by passage through a MnO oxygen-removal column and a Davison 4 Å molecular sieve column. Pentane and toluene were dried using activated alumina columns according to the method described by Grubbs[14] and were additionally vacuum-transferred from Na/K alloy immediately prior to use if employed for catalyst synthesis or catalytic reactions. Ethanol and methanol were distilled from a small amount of sodium under nitrogen, while ether and THF were distilled from sodium benzophenone ketyl. Dichloromethane was distilled before use from CaH_2 under nitrogen. Chloroform-*d* and dichloromethane-d_2 were purchased from Cambridge Isotope Laboratories. Benzene-d_6 and toluene-d_8 (Cambridge Isotope Laboratories; all 99+ atom % D) used for NMR reactions and kinetic measurements were stored in vacuo over Na/K alloy in resealable bulbs and were vacuum-transferred immediately prior to use. All organic starting materials were purchased from Sigma-Aldrich Co. or Fisher Scientific Inc. and were used without further purification unless otherwise stated. All ligands synthesized here were dried overnight on a high-vacuum line. They were then brought into the glovebox, added to a small amount of dry benzene-d_6, degassed overnight on the high-vacuum line again, and stored in the glovebox. Organophosphine oxide- and sulfide-substituted binaphthol ligands **1**,[12e] **4**,[12e] and **7**[12a] and aminoalkene substrates **9**,[3v] **10**,[3e] **11**,[3v] and **12**[3r] were prepared as reported previously. All substrates were dried twice as solutions in benzene-d_6 or toluene-d_8 over freshly activated Davison 4 Å molecular sieves and were degassed by freeze−pump−thaw methods. The substrates were then stored in vacuum-tight storage flasks. The lanthanide complexes $Ln[N(SiMe_3)_2]_3$[15] and $Ln[CH(SiMe_3)_2]_3$[16] (Ln = La, Nd, Sm, Y, Lu, and Sc) were prepared according to published procedures.

Physical and Analytical Measurements. NMR spectra were recorded on a Varian Gemini 300 (300 MHz, ^1H; 75 MHz, ^{13}C), Mercury-400 (FT, 400 MHz, ^1H; 100 MHz, ^{13}C; 126 MHz, ^{31}P), or Inova-500 (500 MHz, ^1H; 125 MHz, ^{13}C) instrument. Chemical shifts (δ) for ^1H, ^{13}C, and ^{31}P are referenced to internal solvent resonances and reported relative to $SiMe_4$ and phosphoric acid, respectively. NMR experiments on air-sensitive samples were conducted in Teflon valve-sealed J. Young tubes. MS studies were conducted on an MS-LCQ Advantage instrument with 70 eV electron impact ionization or chemical ionization using isobutane as the reagent gas. Elemental analyses were performed by Midwest Microlabs, Indianapolis, IN. HPLC analyses were performed using a Waters Breeze system consisting of a model 1525 binary pump, model 77251 manual injector, and model 2487 dual UV/vis detector.

(*R*)-3,3′-Bis(diethylphosphinoylmethyl)-2,2′-bis(methoxymethyl)-1,1′-binaphthol (2a). The procedure was adapted from published procedures.[12e] A solution of diethylphosphine oxide[17] (0.302 g, 2.84 mmol) in THF (14 mL) was treated with NaO^{t}Bu (0.275 g, 2.86 mmol) in THF (7 mL) at 0 °C. The colorless solution was kept stirring at room temperature for 1 h. To this stirring solution was added (*R*)-3,3′-bis(chloromethyl)-2,2′-bis(methoxymethyl)-1,1′-binaphthol[12c] (0.490 g, 1.04 mmol) in THF (6 mL) at −40 °C, and the reaction mixture was allowed to gradually warm to room temperature. After the completion of the reaction in ca. 4 h, a saturated aqueous NH_4Cl solution was added, and the reaction mixture was concentrated to half under vacuum, followed by dilution with ethyl acetate (30 mL). The organic layer was then washed with water (20 mL × 2), and the separated aqueous layer was carefully extracted with ethyl acetate (20 mL × 3). The combined organic layer was then washed with brine (20 mL × 2). After the removal of the solvent, further purification was carried out by flash chromatography (CH_2Cl_2/MeOH, 30:1) to give **2a** (0.332 g, 52.3%) as a colorless oil. Similar to that reported,[14] ^1H NMR ($CDCl_3$, 499.7 MHz, 23 °C): 8.11 (d, J = 2.50 Hz, 2H), 7.90 (d, J = 8.00 Hz, 2H), 7.42 (t, J = 7.50 Hz, 2H), 7.27 (m, 2H), 7.14 (d, J = 8.00 Hz, 2H), 4.39 (d, J = 6.00 Hz, 2H, OCH_2-OCH$_3$), 4.31 (d, J = 6.00 Hz, 2H, OCH_2OCH$_3$), 3.66 (t, J = 14.5

(11) (a) Cotton, S. In *Lanthanide and Actinide Chemistry*; John Wiley & Sons: West Sussex, England, 2006; pp 35−56. (b) Aspinall, H. C. In *Chemistry of the f-Block Elements*; OPA: Amsterdam, The Netherlands, 2001; pp 61−108. (c) Aspinall, H. C.; Moore, S. R.; Smith, A. K. *J. Chem. Soc., Dalton Trans.* **1992**, 153−156. (d) Bradley, D. C.; Ghotra, J. S.; Hart, F. A.; Hursthouse, M. B.; Raithby, P. R. *J. Chem. Soc., Dalton Trans.* **1977**, 1166−1172.

(12) (a) Ichikawa, E.; Suzuki, M.; Yabu, K.; Albert, M.; Kanai, M.; Shibasaki, M. *J. Am. Chem. Soc.* **2004**, *126*, 11808−11809. (b) Hamashima, Y.; Sawada, D.; Nogami, H.; Kanai, M.; Shibasaki, M. *Tetrahedron* **2001**, *57*, 805−814. (c) Takamura, M.; Funabashi, K.; Kanai, M.; Shibasaki, M. *J. Am. Chem. Soc.* **2001**, *123*, 6801−6808. (d) Takamura, M.; Funabashi, K.; Kanai, M.; Shibasaki, M. *J. Am. Chem. Soc.* **2000**, *122*, 6327−6328. (e) Hamashima, Y.; Sawada, D.; Kanai, M.; Shibasaki, M. *J. Am. Chem. Soc.* **1999**, *121*, 2641−2642.

(13) Boehme, C.; Wipff, G. *J. Phys. Chem. A* **1999**, *103*, 6023−6029.

(14) Pangborn, A. B.; Giardello, M. A.; Grubbs, R. H.; Rosen, R. K.; Timmers, F. J. *Organometallics* **1996**, *15*, 1518−1520.

(15) (a) Schuetz, S. A.; Day, V. W.; Sommer, R. D.; Rheingold, A. L.; Belot, J. A. *Inorg. Chem.* **2001**, *40*, 5292−5295. (b) Bradley, D. C.; Ghotra, J. S.; Hart, F. A. *J. Chem. Soc., Dalton Trans.* **1973**, 1021−1023. (c) Alyea, E. C.; Bradley, D. C.; Copperthwaite, R. G. *J. Chem. Soc., Dalton Trans.* **1972**, 1580−1584.

(16) Hitchcock, P. B.; Lappert, M. F.; Smith, R. G.; Bartlett, R. A.; Power, P. P. *J. Chem., Soc., Chem. Commun.* **1988**, 1007−1009.

(17) Hays, H. R. *J. Org. Chem.* **1968**, *33*, 3690−3694.

Hz, 2H, CH_2P(O)Et$_2$), 3.40 (t, J = 14.5 Hz, 2H, CH_2P(O)Et$_2$), 3.04 (s, 6H, OCH$_2$OCH_3), 1.83 (m, 4H, CH_2CH$_3$), 1.72 (m, 4H, CH_2-CH$_3$), 1.23 (m, 12H, CH$_2$CH_3). ^{13}C NMR (CDCl$_3$, 125.7 MHz, 23 °C): δ 133.3 (d, J = 1.51 Hz), 131.4 (d, J = 2.51 Hz), 131.0 (d, J = 3.02 Hz), 128.4, 126.9, 126.4, 126.4, 125.8, 125.7, 125.5, 99.9, 57.6, 30.3 (d, J = 59.4 Hz), 20.4 (m), 6.0. ^{31}P NMR (CDCl$_3$, 162.0 MHz, 23 °C): 51.47. MS m/z 633 (M + Na$^+$).

(*R*)-3,3′-Bis(diethylphosphinoylmethyl)-1,1′-binaphthol (2). The procedure was adapted from published procedures.[12e] Compound **2a** (0.332 g, 0.544 mmol) was dissolved in a methanol/CH$_2$-Cl$_2$ mixture (4.0 mL/2.0 mL). A catalytic amount of TsOH (monohydrate, 0.0550 g) was then added, and the resulting solution was stirred at room temperature overnight. Most of the solvent was next removed in vacuo, and the residue was diluted with 20 mL of ethyl acetate. The solution was then washed with water (20 mL × 2), and the aqueous layer was extracted with ethyl acetate (30 mL × 3). The combined organic layer was washed with brine and dried over Na$_2$SO$_4$. After filtration and evaporation of the filtrate, the crude product was further purified by recrystallization (CH$_2$Cl$_2$/Et$_2$O) to give **2** (0.150 g, 52.8%) as a white powder. ^{1}H NMR (CDCl$_3$, 499.7 MHz, 23 °C): δ 8.29 (s, 2H, OH), 7.81 (d, J = 8.50 Hz, 2H), 7.78 (s, 2H), 7.32 (t, J = 7.50 Hz, 2H), 7.22 (t, J = 7.50 Hz, 2H), 7.11 (d, J = 8.50 Hz, 2H), 3.47 (m, 4H, CH_2P(O)-Et$_2$), 1.84 (m, 8H, CH_2CH$_3$), 1.21 (m, 12H, CH$_2$CH_3). ^{13}C NMR (CDCl$_3$, 125.7 MHz, 23 °C): δ 151.7 (d, J = 3.02 Hz), 133.7 (d, J = 2.26 Hz), 130.9 (d, J = 6.03 Hz), 129.3 (d, J = 1.51 Hz), 127.8, 126.7, 125.3, 124.0, 122.7 (d, J = 8.42 Hz), 118.2, 32.2 (d, J = 60.3 Hz), 20.3 (dd, J = 65.7, 10.7 Hz), 6.01. ^{31}P NMR (CDCl$_3$, 162.0 MHz, 23 °C): δ 56.32. ^{1}H NMR (benzene-d_6, 499.7 MHz, 23 °C, only slightly soluble): δ 10.34 (s, 2H, OH), 7.79 (d, J = 8.00 Hz, 2H), 7.68 (s, J = 8.00 Hz, 2H), 7.34, 7.29, 7.24, 2.75 (d, 4H, J = 12.5 Hz, CH_2P(O)Et$_2$), 1.08 (m, 8H, CH_2CH$_3$), 0.64 (m, 12H, CH$_2$CH_3). ^{31}P NMR (benzene-d_6, 162.0 MHz, 23 °C): 55.45. MS m/z 545 (M + Na$^+$). Anal. Calcd for C$_{30}$H$_{36}$O$_4$P$_2$: C, 68.95; H, 6.94. Found: C, 68.89; H, 6.91.

(*R*)-3,3′-Bis[di(*tert*-butyl)phosphinoylmethyl]-2,2′-bis(methoxymethyl)-1,1′-binaphthol (3a). A solution of di(*tert*-butyl)phosphine oxide (0.250 g, 1.54 mmol) in THF (8 mL) was treated with NaO^t-Bu (0.148 g, 1.54 mmol) in THF (4 mL) at 0 °C. The clear solution was stirred at room temperature for 0.5 h. To this clear solution was then added (*R*)-3,3′-bis(chloromethyl)-2,2′-bis(methoxymethyl)-1,1′-binaphthol (0.265 g, 0.562 mmol) in THF (4 mL) at −40 °C, and the reaction mixture was gradually warmed to room temperature. After the reaction was allowed to stand overnight, a saturated aqueous NH$_4$Cl solution was added, and the reaction mixture was concentrated to half on the rotary evaporator, followed by dilution with 25 mL of ethyl acetate. The organic layer was then washed with water (15 mL × 2) and the separated aqueous phase carefully extracted with ethyl acetate (15 mL × 3). The combined organic layer was next washed with brine (15 mL × 2), and the solvent removed by rotary evaporation. Further purification was carried out by flash chromatography (CH$_2$Cl$_2$/MeOH, 15:1) to give **3a** (0.340 g, 83.7%) as a white powder. ^{1}H NMR (CDCl$_3$, 499.7 MHz, 23 °C): δ 8.52 (2H), 7.93 (d, J = 8.00 Hz, 2H), 7.38 (t, J = 7.00 Hz, 2H), 7.20 (t, J = 7.50 Hz, 2H), 7.08 (d, J = 8.50 Hz, 2H), 4.41 (d, J = 6.50 Hz, 2H, OCH_2OCH$_3$), 4.32 (d, J = 6.00 Hz, 2H, OCH_2OCH$_3$), 3.73 (m, 2H, CH_2P(O)^{t}Bu$_2$), 3.38 (t, J = 15.0 Hz, 2H, CH_2P(O)^{t}Bu$_2$), 3.15 (s, 6H, OCH$_2$OCH_3), 1.30 (m, 36H, C(CH_3)$_3$). ^{31}P NMR (CDCl$_3$, 162.0 MHz, 23 °C): δ 61.04. MS m/z 745 (M + Na$^+$).

(*R*)-3,3′-Bis[di(*tert*-butyl)phosphinoylmethyl]-1,1′-binaphthol (3). Compound **3a** (0.340 g, 0.471 mmol) was dissolved in the mixture of methanol/CH$_2$Cl$_2$ (4.0 mL/2.0 mL). A catalytic amount of TsOH (monohydrate, 0.0505 g) was next added and the reaction mixture stirred at room temperature for 3 h. Most of the solvent was then removed in vacuo, and the residue was diluted with ethyl acetate. The resulting solution was washed with water (20 mL × 2), and the aqueous layer was extracted with ethyl acetate (30 mL × 3). The combined organic layer was washed with brine and dried over Na$_2$SO$_4$. After filtration, the crude product was further purified by recrystallization (CH$_2$Cl$_2$/Et$_2$O) to give **3** (0.241 g, 80.7%) as a white powder. ^{1}H NMR (CD$_2$Cl$_2$, 499.7 MHz, 23 °C): δ 10.6 (s, 2H, OH), 7.81 (d, J = 8.00 Hz, 2H), 7.75 (s, 2H), 7.30 (t, J = 7.50 Hz, 2H), 7.19 (t, J = 7.50 Hz, 2H), 7.06 (d, J = 8.50 Hz, 2H), 3.74 (m, 2H, CH_2P(O)^{t}Bu$_2$), 3.48 (m, 2H, CH_2P(O)^t-Bu$_2$), 1.38 (m, 36H, C(CH_3)$_3$). ^{13}C NMR (CD$_2$Cl$_2$, 125.7 MHz, 23 °C): δ 152.7, 133.9, 130.2 (s), 130.2, 129.0, 127.4, 125.9, 125.0, 123.3, 120.9, 53.68 (m), 36.58 (m), 6.01 (d, J = 69.5 Hz). ^{31}P NMR (CD$_2$Cl$_2$, 162.0 MHz, 23 °C): δ 69.44. MS m/z 635 (M + H$^+$). Anal. Calcd for C$_{38}$H$_{52}$O$_4$P$_2$: C, 71.90; H, 8.26. Found: C, 71.81; H, 8.13.

(*R*)-3,3′-Bis(dibenzylphosphinoylmethyl)-2,2′-bis(methoxymethyl)-1,1′-binaphthol (5a). A solution of dibenzylphosphine oxide[18] (0.659 g, 2.86 mmol) in THF (14 mL) was treated with NaO^{t}Bu (0.275 g, 2.86 mmol) in THF (7 mL) at 0 °C. The clear solution was then stirred at room temperature for 1 h. To this clear solution was added (*R*)-3,3′-bis(chloromethyl)-2,2′-bis(methoxymethyl)-1,1′-binaphthol (0.490 g, 1.04 mmol) in THF (6 mL) at −40 °C, and the reaction mixture was gradually warmed to room temperature. After the completion of the reaction in ca. 2 h, a saturated aqueous NH$_4$Cl solution was added, and the reaction mixture was concentrated by rotary evaporation to half, followed by dilution with ethyl acetate (30 mL). The organic layer was washed with water (20 mL × 2), and the separated aqueous layer carefully extracted with ethyl acetate (20 mL × 3). The combined organic phase was then washed with brine (20 mL × 2). After the removal of the solvent in vacuo, further purification was carried out by flash chromatography (CH$_2$Cl$_2$/MeOH, 30:1) to give **5a** (0.711 g, 79.6%) as a white solid. ^{1}H NMR (CDCl$_3$, 499.7 MHz, 23 °C): δ 8.06 (d, J = 2.50 Hz, 2H), 7.88 (d, J = 8.50 Hz, 2H), 7.42 (t, J = 7.00 Hz, 2H), 7.31 (m, 2H), 7.19 (d, J = 8.50 Hz, 2H), 4.35 (d, J = 6.00 Hz, 2H, OCH_2OCH$_3$), 4.27 (d, J = 6.00 Hz, 2H, OCH_2OCH$_3$), 3.56 (m, 2H, CH_2P(O)Et$_2$), 3.26 (m, 2H, CH_2P(O)Et$_2$), 3.14 (m, 8H, CH_2Ph), 2.84 (s, 6H, OCH$_2$OCH_3). ^{13}C NMR (CDCl$_3$, 125.7 MHz, 23 °C): δ 152.7 (d, J = 4.52 Hz), 133.3 (d, J = 1.81 Hz), 132.2 (m), 131.0 (d, J = 2.72 Hz), 130.2 (d, J = 4.53 Hz), 130.0 (d, J = 4.53 Hz), 128.5, 127.1 (m), 127.0, 125.8 (m), 99.7, 57.2, 35.6 (m), 30.6 (d, J = 61.0 Hz). ^{31}P NMR (CDCl$_3$, 162.0 MHz, 23 °C): δ 42.54. MS m/z 881 (M + Na$^+$).

(*R*)-3,3′-Bis(dibenzylphosphinoylmethyl)-1,1′-binaphthol (5). Compound **5a** (0.711 g, 0.828 mmol) was dissolved in a mixture of methanol/CH$_2$Cl$_2$ (8.0 mL/8.0 mL). A catalytic amount of TsOH (monohydrate, 0.0800 g) was then added and the reaction mixture stirred at room temperature for 3.5 h. Most of the solvent was then removed in vacuo, and the residue was diluted with ethyl acetate. The resulting solution was washed with water (20 mL × 2), and the aqueous layer was extracted with ethyl acetate (30 mL × 3). The combined organic layer was washed with brine and dried over Na$_2$SO$_4$. After filtration and removal of the solvent by rotary evaporation, the crude product was further purified by recrystallization (CH$_2$Cl$_2$/Et$_2$O) to give **5** (0.551 g, 86.4%) as a white powder. ^{1}H NMR (CDCl$_3$, 499.7 MHz, 23 °C): δ 8.00 (s, 2H, OH), 7.76 (d, J = 8.50 Hz, 2H), 7.70 (s, 2H), 7.27 (m, 22H), 7.06 (d, J = 8.50 Hz, 2H), 3.41 (m, 2H, CH_2P(O)Bn$_2$), 3.32 (m, 2H, CH_2P(O)-Bn$_2$), 3.21 (m, 8H, CH_2Ph). ^{13}C NMR (CDCl$_3$, 125.7 MHz, 23 °C): δ 151.4 (d, J = 3.90 Hz), 133.6 (d, J = 2.26 Hz), 131.5 (d, J = 6.05 Hz), 131.4 (m), 120.1 (d, J = 5.42 Hz), 129.2, 129.0 (m), 127.8, 127.3 (d, J = 2.27 Hz) 126.7, 125.1, 124.0, 122.0, 121.9, 117.94 (d, J = 2.39 Hz), 35.9 (d, J = 16.8 Hz), 35.4 (d, J = 17.5 Hz), 32.3 (d, J = 60.4 Hz). ^{31}P NMR (CDCl$_3$, 162.0 MHz, 23 °C): δ 47.50. ^{1}H NMR (benzene-d_6, 499.7 MHz, 23 °C, only slightly soluble): δ 9.58 (s, 2H, OH), 7.69 (d, J = 8.50 Hz, 2H), 7.52 (s,

(18) Clément, J.-L.; Fréjaville, C.; Tordo, P. *Res. Chem. Intermed.* **2002**, *28*, 175−180.

Table 1. Summary of the Crystal Structure Data for Compounds 1, 2, 3, and 8

	1·pentane ($C_{51}H_{48}O_4P_2$)	**2** ($C_{30}H_{36}O_4P_2$)	**3**·toluene ($C_{45}H_{60}O_4P_2$)	**8**·6toluene ($C_{180}H_{1502}La_2O_{12}P_6$)
fw	786.83	522.53	726.87	2968.64
cryst syst	monoclinic	monoclinic	triclinic	hexagonal
space group	*C*2	$P2_1$	*P*1	$P6_3$
a, Å	16.114(3)	8.7568(9)	11.5165(15)	31.7444(16)
b, Å	18.939(3)	17.2784(17)	11.7891(15)	31.7444(16)
c, Å	25.987(5)	9.5484(10)	16.411(2)	25.393(3)
α, deg			108.081(2)	
β, deg	98.317(4)	104.529(2)	101.365(2)	
γ, deg			90.766(2)	
V, Å^3	7847(2)	1398.5(2)	2069.9(5)	22160(3)
Z	8	2	2	6
d_{cacd}, g/cm^3	1.167	1.241	1.166	1.086
cryst size, mm^3	0.10 × 0.06 × 0.06	0.40 × 0.35 × 0.10	0.35 × 0.33 × 0.29	0.45 × 0.06 × 0.05
color, habit	colorless, needle	colorless, plate	colorless, cube	colorless, needle
temp, °C			-120	
μ, cm^{-1}	1.60	1.88	1.45	6.99
θ range, deg	0.79−28.48	2.20−28.78	1.34−28.73	0.74−28.92
radiation	graphite monochromator; Mo Kα, = 0.71073 Å			
intensities (uniq, R_i)	23 626 (15 603, 0.0661)	12 937 (6346, 0.0263)	19 142 (16 574, 0.0192)	189 306, (36 274, 0.2384)
R (R_w^2 all data)	0.0700 (0.1489)	0.0508 (0.1241)	0.0535 (0.1370)	0.0586 (0.1386)
no. of params	979	331	949	1423
goodness-of-fit on F^2	1.001	1.046	1.013	0.700
max., min. density in Δ*F* map, e/Å^3	0.644, −0.331	0.744, −0.253	0.547, −0.316	0.756, −0.442

[a] $R_w^2 = [\sum w(F_o^2 - F_c^2)^2/\sum w(F_o^2)^2]^{1/2}$; $R = \sum||F_o| - |F_c||/\sum|F_o|$; $w = 1/[\sigma^2(F_o^2) + (aP)^2 + bP]$; $P = [2F_c^2 + \mathrm{Max}(F_o^2, 0)]/3$.

J = 8.50 Hz, 2H), 7.29, 7.27, 7.23, 6.96, 2.93 (d, 4H, J = 12.5 Hz, CH_2P(O)Et$_2$), 2.66 (m, 22H). ^{31}P NMR (benzene-d_6, 162.0 MHz, 23 °C): δ 46.87. MS *m*/*z* 771 (M + H$^+$). Anal. Calcd for $C_{50}H_{44}O_4P_2$: C, 77.91; H, 5.75. Found: C, 77.90; H, 5.80.

(*R*)-3,3′-Bis(diethoxylphosphinoylmethyl)-2,2-bis(methoxymethyl)-1,1′-binaphthol (6a). A solution of diethoxylphosphine oxide (0.392 g, 2.84 mmol) in THF (14 mL) was treated with NaO^t-Bu (0.275 g, 2.86 mmol) in THF (7 mL) at 0 °C. The clear solution was next stirred at room temperature for 1 h. To this clear solution was added (*R*)-3,3′-bis(chloromethyl)-2,2′-bis(methoxymethyl)-1,1′-binaphthol (0.490 g, 1.04 mmol) in THF (6 mL) at −40 °C, and the reaction mixture was gradually warmed to room temperature. After the reaction mixture had been refluxed overnight, a saturated aqueous NH_4Cl solution was added, and the reaction mixture was concentrated to half, followed by dilution with ethyl acetate (30 mL). The organic layer was then washed with water (20 mL × 2), and the separated aqueous layer was carefully extracted with ethyl acetate (20 mL × 3). The combined organic layer was washed with brine (20 mL × 2). After the removal of the solvent by rotary evaporation, further purification was carried out by flash chromatography (CH_2Cl_2/MeOH, 30:1) to give **6a** (0.496 g, 70.7%) as a light yellow, thick oil. ^{1}H NMR ($CDCl_3$, 499.7 MHz, 23 °C): δ 8.12 (d, J = 3.00 Hz, 2H), 7.86 (d, J = 8.00 Hz, 2H), 7.39 (t, J = 7.00 Hz, 2H), 7.23 (m, 2H), 7.13 (d, J = 8.00 Hz, 2H), 4.60 (d, J = 5.50 Hz, 2H, OCH_2OCH$_3$), 4.49 (d, J = 5.50 Hz, 2H, OCH_2-OCH$_3$), 4.11(m, 8H, OCH_2CH$_3$), 3.57 (m, 4H, CH_2P(O)Et$_2$), 2.93 (s, 6H, OCH$_2$OCH_3), 1.31 (m, 12H, OCH$_2$CH_3). ^{13}C NMR ($CDCl_3$, 125.7 MHz, 23 °C): δ 152.7 (d, J = 7.56 Hz), 133.4 (d, J = 2.39 Hz), 131.1 (d, J = 6.93 Hz), 130.7 (d, J = 3.78 Hz), 128.0, 126.5, 126.0, 125.8, 125.7, 125.6 (d, J = 2.27 Hz), 125.4, 99.4, 64.3 (m), 56.9, 28.2, 27.1, 16.6 (d, J = 6.05 Hz). ^{31}P NMR ($CDCl_3$, 162.0 MHz, 23 °C): δ 27.81. MS *m*/*z* 697 (M + Na$^+$).

(*R*)-3,3-Bis(diethoxylphosphinoylmethyl)-1,1-binaphthol (6). Compound **6a** (0.496 g, 0.735 mmol) was dissolved in the mixture of ethanol/CH_2Cl_2 (6.0 mL/6.0 mL). A catalytic amount of TsOH (monohydrate, 0.0705 g) was added, and the reaction mixture was then refluxed at 40 °C overnight. Next, most of the solvent was removed in vacuo, and the residue was diluted with ethyl acetate. The resulting solution was washed with water (20 mL × 2), and the aqueous layer was extracted with ethyl acetate (30 mL × 3). The combined organic layer was washed with brine and dried over Na_2SO_4. After filtration and evaporation of the solvent, the crude product was further purified by flash chromatography (CH_2Cl_2/MeOH, 30:1) to give **6** (0.319 g, 74.0%) as a light yellow powder. ^{1}H NMR (benzene-d_6, 499.7 MHz, 23 °C): δ 8.64 (s, 2H, O*H*), 7.70 (d, J = 8.00 Hz, 2H), 7.60 (d, J = 3.00 Hz, 2H), 7.45 (t, J = 8.50 Hz, 2H), 7.16 (t, J = 8.00 Hz, 2H), 7.04 (t, J = 7.50 Hz, 2H), 3.73 (m, 8H, OCH_2CH$_3$), 3.24 (m, 4H, CH_2P(O)Et$_2$), 0.87 (m, 12H, OCH$_2$CH_3). ^{13}C NMR (benzene-d_6, 125.7 MHz, 23 °C): δ 152.3 (d, J = 3.91 Hz), 134.5 (d, J = 2.27 Hz), 131.0 (d, J = 9.20 Hz), 129.7 (d, J = 3.02 Hz), 126.5, 125.7, 123.8, 122.3 (d, J = 9.20 Hz), 119.7, 62.7 (dd, J = 63.5, 6.93 Hz), 30.1 (d, J = 65.0 Hz), 16.2. ^{31}P NMR (benzene-d_6, 162.0 MHz, 23 °C): δ 30.04; MS *m*/*z* 587 (M + H$^+$). Anal. Calcd for $C_{30}H_{36}O_8P_2$: C, 61.43; H, 6.19. Found: C, 61.33; H, 6.31.

Small-Scale Preparation of La$_2${(*R*)-BINOL-[P(O)Ph$_2$]$_2$}$_3$ (8). A mixture of La[N(SiMe$_3$)$_2$]$_3$ (10.0 mg, 0.0161 mmol) and (*R*)-3,3′-bis(diphenylphosphinoylmethyl)-1,1′-binaphthol (20.0 mg, 0.0280 mmol) was dissolved in benzene-d_6 (0.60 mL) in the glovebox. The excess of ligand **2**, which was not soluble, was filtered off to afford a clear filtrate, which was allowed to stand overnight at room temperature. The volatiles were then removed in vacuo to give a light brown solid (17.1 mg, 87.7%). ^{1}H NMR (benzene-d_6, 499.7 MHz, 23 °C): δ 7.91, 7.44, 7.23, 7.09, 7.02, 6.82, 6.66, 7.02, 6.40, 6.23 (m, total 10H), 2.95 (m, 1H, CH_aH$_b$), 2.83 (m, 1H, CH$_a$CH_b). ^{13}C NMR (benzene-d_6, 125.6 MHz, 23 °C): δ 162.3 (d, J = 2.51 Hz), 136. 6, 136.1, 135.8, 132.5 (d, J = 9.67 Hz), 131.2 (d, J = 9.55 Hz), 131.1, 130.6, 130.1 (d, J = 8.54 Hz), 128.8 (d, J = 9.17 Hz), 126.8, 126.6, 124.0, 119.5, 118.7, 35.91 (d, J = 67.8 Hz, *C*H$_2$). ^{31}P NMR (benzene-d_6, 162.0 MHz, 23 °C): δ 40.99. Anal. Calcd for $C_{138}H_{102}La_2O_{12}P_6$: C, 68.61; H, 4.26. Found: C, 68.29; H, 4.76.

X-ray Crystallographic Studies of 1, 2, 3, and 8. Organophosphine oxide-substituted binaphthol crystals **1**, **2**, and **3** were grown from mixed pentane/CH_2Cl_2 or toluene/CH_2Cl_2 solutions, while lanthanum complex **8** was obtained by slow diffusion of pentane into its toluene solution. Suitable crystals were mounted on glass fibers with Paratone-N oil (Exxon) and positioned in a Bruker SMART-1000 CCD diffractometer equipped with a Nicolet LT low-temperature device. Crystal data collection parameters are summarized in Table 1. Data were processed using the SAINT software package from Bruker, and all calculations were performed using

Scheme 3. Synthesis of Organophosphine Oxide-Substituted Binaphthol Ligands

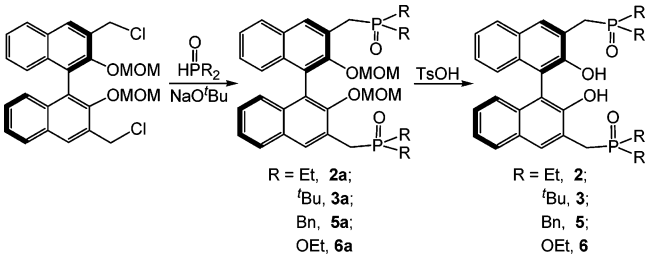

the Bruker SHELXTL[19] crystallographic software package. Absorption corrections were applied with the Bruker SADABS program.[19] The structures were solved by direct methods[20] and expanded using Fourier techniques.[20] The non-hydrogen atoms were refined anisotropically. Hydrogen atoms were included but not refined. The program SQUEEZE was applied to structure **8** to remove the intensity contributions from the mostly disordered toluene solvent molecules.[21] The final refinement of the structure of **8** was carried out using the SQUEEZE modified intensities. The intensity data factor here was high ($R_{int} = 0.2384$) and goodness-of-fit on F^2 was still somehow low due to the poor quality of the crystals.

Typical NMR-Scale Catalytic Reactions. In the glovebox, the lanthanide precursor $Ln[N(SiMe_3)_2]_3$ (7.1 μmol) and neutral organophosphine oxide-substituted binaphthol (7.8 μmol) were weighed into a vial, and 500 μL of benzene-d_6 was added by syringe. The solution was mixed to yield a homogeneous, clear solution and then transferred to a J. Young NMR tube equipped with a Teflon valve. The tube was then closed, taken out from the glovebox, and shaken by hand. When an internal standard was used, 300 μL of benzene-d_6 and a solution of the internal NMR integration standard Si(*p*-$CH_3C_6H_4)_4$ in benzene-d_6 (35 mM, 200 μL, 7 μmol) was added by syringe before sealing the NMR tube. The ensuing in situ generation of the precatalyst was monitored by ^{1}H NMR, and the complete consumption of the starting $Ln[N(SiMe_3)_2]_3$ complex was observed to occur essentially instantaneously. The precatalyst solution was then allowed to stand at room temperature overnight. The substrate (ca. 1 M in benzene-d_6, 0.15 mL, 20-fold molar excess) was added by syringe to the catalyst solution in the glovebox. The NMR tube was then frozen at −78 °C until the time for in situ NMR analysis and brought to the desired temperature, and the ensuing hydroamination/cyclization reaction was monitored by ^{1}H NMR spectroscopy. After the reaction was complete, the reaction mixture was freeze−pump−thaw degassed and the volatiles were vacuum-transferred into a separate NMR tube. The solvent was next removed on a rotary evaporator at 0 °C to afford the hydroamination product. Alternatively, for nonvolatile hydroamination products, filtration of the reaction mixture through a small plug of silica gel removed the catalyst. The silica gel was then rinsed several times with Et_2O (25 mL), and the fractions were combined and evaporated under reduced pressure to afford the HA product.

Determination of Enantiomeric Excess and Absolute Configuration. The values for the enantiomeric excesses of the chiral products were determined by chiral stationary phase HPLC analysis using a Regis (*S,S*)-Whelk O1 or Regis (*R,R*)-*β*-Gem1 column (i.d. = 4.6 mm, length = 250 mm, and particle size = 5 mm). The analysis methods and HPLC conditions are the same as reported previously.[3e] The 2-substituted azacyclic hydroamination products were derivatized as 1-naphthoyl amides for HPLC analysis by treating with 1-naphthoyl chloride and Et_3N in CH_2Cl_2/Et_2O.[3e]

Kinetic Studies of Hydroamination/Cyclization. In a typical experiment, an NMR sample was prepared as described above (see Typical NMR-Scale Catalytic Reactions) but maintained at −78 °C until kinetic measurements were begun. After substrate addition, the sample tube was inserted into the probe of the INOVA-500 spectrometer, which had been previously set to the desired temperature ($T \pm 0.2$ °C; checked with a methanol or ethylene glycol temperature standard). A single acquisition (nt = 1) with a 45° pulse was used during data acquisition to avoid saturation. The substrate concentration was measured from the olefinic peak area, A_s, standardized to A_l, the methyl peak area of the Si(*p*-$CH_3C_6H_4)_4$ internal standard. The turnover frequency, N_t (h^{-1}), was calculated from the least-squares-determined slope (m) according to eq 3, where $[catalyst]_0$ is the initial concentration of the precatalyst.

$$[\text{substrate}] = mt + [\text{substrate}]_0 \quad (2)$$

$$N_t(h^{-1}) = -\frac{60\ \text{min}}{\text{h}} \times \frac{m}{[\text{catalyst}]_0} \quad (3)$$

Results and Discussion

We previously reported C_2-symmetric bis(oxazolinato)lanthanide catalysts for intramolecular enantioselective hydroamination/cyclization.[3e] In a continued quest for new, nonepimerizable chiral ligand designs for lanthanide ion-mediated hydroamination, configurationally stable chiral phosphine oxide/sulfide-modified binaphthol ligands were developed for this study. This section first presents synthetic routes to the various organophosphine oxide/sulfide-substituted binaphthol ligand precursors {(*R*)-H_2BINOL-[P(O)R_2]$_2$, R = Ph, Et, ^{t}Bu, 3,5-xylyl, Bn, and OEt; and (*R*)-H_2BINOL-[P(S)Ph_2]$_2$} and their structural characterization by a variety of techniques, including single-crystal X-ray diffraction. Next, in situ protonolytic generation of lanthanide binaphtholate catalysts and the X-ray crystal structure of a La_2{(*R*)-BINOL-[P(O)Ph_2]$_2$}$_3$ byproduct are discussed. Finally, systematic optimization of these in situ-generated catalysts with regard to catalytic enantioselective hydroamination/cyclization is described, including effects of lanthanide ion size and ligand architectures on catalytic rates and enantioselectivity, as well as kinetic studies suggesting mechanistic scenarios and catalyst molecularities.

Organophosphine Oxide/Sulfide-Substituted Binaphtholate Ligand Synthesis. The family of the substituted binaphthol ligands examined in this study is shown in Scheme 2. To explore the effects of the binaphtholate ligand substitution pattern on rare earth metal complex catalytic activity and selectivity, several new binaphthol ligands were synthesized. Ligands **1**, **4**, and **7** were prepared according to the general procedures reported by Shibasaki et al.,[12] while ligands **2**, **3**, **5**, and **6** were synthesized following the pathways summarized in Scheme 3. The corresponding phosphine oxide reagents either are commercially available or were prepared by literature procedures. The phosphine oxide reagents were first deprotonated with sodium *tert*-butyloxide (Scheme 3), then condensed with protected chloromethylbinaphthol, and then deprotected to afford the corresponding ligand. During the deprotection process for intermediate **6a**, rapid scrambling of the ligand ethoxy groups with the methanol solvent was observed, affording a mixed ethoxy-/methoxy-phosphine oxide substituted ligand precursor as shown in Scheme 4. Similar exchange processes have been

(19) *Saint-Plus and Shelxtl for Windows: Crystal Structure Analysis Package*; Bruker Analytical X-ray Instruments, Inc.: Madison, WI, 1997.
(20) Sheldrick, G. M. *SHELXTL (version 6.14)*; Bruker Analytical X-ray Instruments, Inc.: Madison, WI, 2003.
(21) Spek, A. L. *J. Appl. Crystallogr.* **2003**, *36*, 7−13.

Scheme 4. Alkoxy Group Exchange in Ethoxy-Substituted Phosphine Oxides

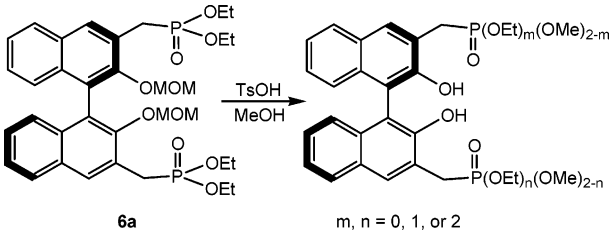

6a m, n = 0, 1, or 2

observed in other alkoxy-substituted phosphine oxides[22] and are avoided by using the corresponding dry alcohol as the deprotection solvent.

Molecular Structures of Ligands 1, 2, and 3. Crystals of ligand **1** were grown by slow cooling of pentane/CH_2Cl_2 solutions, while crystals of **2** and **3** were grown by slow evaporation of toluene/CH_2Cl_2 solutions. The crystal structure of ligand precursor **1** contains a disordered pentane molecule, compound **2** is solvent-free, and **3** has one toluene per substituted binaphthol molecule. Molecular drawings of ligand precursors **1**, **2**, and **3** are shown in Figures 1, 2, and 3, respectively. Pertinent bond lengths and angles are summarized in Table 2.

All three ligand precursors crystallize in chiral space groups with each molecule present as the *R* enantiomer. Structure **3** crystallizes in space group *P*1, which is not common for conventional achiral and racemic molecules. In the structure of ligand precursor **1** (Figure 1), there are two unique molecules within each unit cell, each having different binaphthol dihedral angles of 64.7° and 121.3°. Rather different dihedral angles are also observed in the structure of **3**, illustrating the diverse possible bite angles of the two phosphine oxide moieties and the conformationally flexible nature of these ligands. Such flexibility should allow the ligands to chelate lanthanide ions more closely. The oxygen atoms of the phosphine oxide moieties are engaged in strong hydrogen-bonding interactions with the binaphthol hydroxyl groups. The O−H···O hydrogen-bonding distances (1.79−1.90 Å) are typical for phosphine oxide hydrogen bonds, which generally lie in the 1.40−2.10 Å range.[23] Unlike **1** and **3**, structure **2** is solvent-free and has only one unique molecule in the unit cell. The binaphthol dihedral angle is 91.2°, revealing the two naphthyl planes to be almost perpendicular. The various dimensions of the phosphine oxide substituents do not significantly alter the dimensions of the seven-membered hydrogen-bonded ring structures. Structure **3** also has two unique molecules in each cell with binaphthol dihedral angles of 80.6° and 118.9°, an angle range that is smaller than in **1**. These structures are the first reported for free organophosphine oxide-substituted binaphthol ligands, and only a potassium salt of an organophosphine oxide-substituted binaphthyl crown ether has been previous reported.[24]

In Situ Generation of Precatalysts and the Structure of Byproduct Complex 8. Reactions between the present organophosphine oxide/sulfide-substituted binaphthols and the diamagnetic and paramagnetic homoleptic lanthanide amides {Ln[N(SiMe$_3$)$_2$]$_3$, Ln = La, Nd, Sm, Y, Lu, and Sc} were monitored in situ by both ^{1}H and ^{31}P NMR.[25] At room temperature, immediate protonolysis of two of the bulky bis(trimethyl)silylamido ligands by the free binaphthol hydroxyl groups is observed (eq 4). The ^{1}H NMR spectra in benzene-d_6

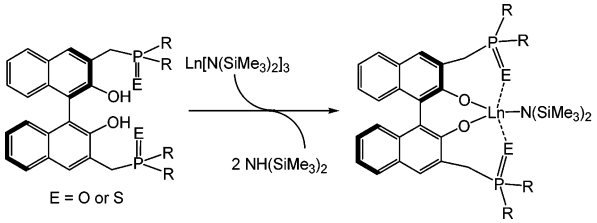

(4)

reveal instantaneous disappearance of the hydroxyl proton signal, generation of the free bis(trimethy)silylamine fingerprints, and displacements of other neutral ligand resonance positions as soon as metal and ligand reagents are combined in benzene-d_6 (Figure 4). Varying ^{31}P NMR shifts from the free ligand positions are observed, in good agreement with literature-reported simple 4f^n lanthanide phosphine oxide complexes,[26] such as in (Ph$_3$PO)-La[N(SiMe$_3$)$_2$]$_2$PPh$_2$.[26a] Depending on the magnetic properties of the coordinated Ln^{3+} ion, the ^{31}P NMR exhibits a modest shift of δ+ 4.77 from 36.23 ppm for the neutral ligand **1** to δ 41.00 ppm after 1:1.1 reaction with La[N(SiMe$_3$)$_2$]$_3$ (Figure 5), or a large shift of δ −33.72 ppm (δ 36.23 to −2.51 ppm) in 1:1.1 reaction of **1** with Nd[N(SiMe$_3$)$_2$]$_3$. In the 1:1.1 reaction of **1** with Sm[N(SiMe$_3$)$_2$]$_3$, a ^{31}P shift of δ +14.51 ppm from δ 36.23 to δ 50.74 ppm is observed. In all cases, a single ^{31}P resonance is observed for the Ln[N(SiMe$_3$)$_2$]$_3$ reaction product, indicating magnetically equivalent −P(O)R$_2$ coordination sites or rapid exchange between nonequivalent sites. For the 1:1.1 reaction between Y[N(SiMe$_3$)$_2$]$_3$ and **1**, characteristic $^3J_{P,Y}$ = 3.7 Hz[26] coupling is observed (^{89}Y, I = 1/2, and natural abundance = 100%[27]), and a downfield shift to δ 42.81 ppm is observed in the ^{31}P NMR spectrum. Observation of $^3J_{P,Y}$ indicates any intermolecular exchange of Y^{3+} between ligand molecules is slow versus the magnitude of $^3J_{P,Y}$. That coordinated ligand ^{31}P NMR chemical shifts do not change significantly from these values and that $^3J_{P,Y}$ does not change significantly in magnitude during the course of catalytic hydroamination argues that the phosphine oxide units remain predominantly bound to the lanthanide ions, even with the introduction of excess amine substrate (Figures 4 and 5).

Far smaller ^{31}P shift displacements are observed when the Ln[N(SiMe$_3$)$_2$]$_3$ reagents react with phosphine sulfide ligand **7**.

(22) (a) Corbridge, D. E. C. In *Phosphorus: An Outline of its Chemistry, Biochemistry, and Technology*; Elsevier: New York, 1978; p 199. (b) Hall, N.; Price, R. *J. Chem. Soc., Perkin Trans. 1* **1979**, 2873−2877. (c) Mikolajczyk, M.; Midura, W. H.; Schmutzler, R.; Schiebel, H.-M.; Schulze, P. *New J. Chem.* **2001**, *25*, 1073−1077. (d) Skropeta, D.; Schmidt, R. R. *Tetrahedron: Asymmetry* **2003**, *14*, 265−273.

(23) (a) Gavryushin, A.; Polborn, K.; Knochel, P. *Tetrahedron: Asymmetry* **2004**, *15*, 2279−2288. (b) Terent'eva, S. A.; Nikolaeva, I. L.; Burilov, A. R.; Kharitonov, D. I.; Popova, E. V.; Pudovik, M. A.; Litvinov, I. A.; Gubaidullin, A. T.; Konovalov, A. I. *Russ. J. Gen. Chem.* **2001**, *71*, 389−395. (c) Jetti, R. K. R.; Weiss, H.-C.; Thalladi, V. R.; Boese, R.; Nangia, A.; Desiraju, G. R. *Acta Crystallogr.* **1999**, *C55*, 1530−1533. (d) Etter, M. C.; Gillard, R. D.; Gleason, W. B.; Rasmussen, J. K.; Duerst, R. W.; Johnson, R. B. *J. Org. Chem.* **1986**, *51*, 5405−5408. (e) Gramstad, T.; Husebye, S.; Maartmann-Moe, K. *Acta Chem. Scand., B* **1986**, *B40*, 26−30. (f) Buss, A. D.; Cruse, W. B.; Kennard, O.; Warren, S. *J. Chem. Soc., Perkins Trans. 1* **1984**, 243−247.

(24) Knobler, C. B.; Maverick, E. F.; Trueblood, K. N.; Helgeson, R. C.; Cram, D. J. *Acta Crystallogr.* **1986**, *C42*, 156−158.

(25) (a) Bertini, I.; Luchinat, C.; Parigi, G. In *Solution NMR of Paramagnetic Molecules: Applications to Metallobiomolecules and Models*, 1st ed.; Elsevier: Amsterdam, The Netherlands, 2001. (b) Bertini, I.; Luchinat, C. *NMR of Paramagnetic Substances*; Elsevier: Amsterdam, Netherlands, 1996. (c) Kaupp, M.; Bühl, M.; Malkin, V. G. *Calculation of NMR and EPR Parameters: Theory and Application*; Wiley-VCH: Weinheim, Germany, 2004.

(26) (a) Aspinall, H. C.; Bradley, D. C.; Sales, K. D. *J. Chem. Soc., Dalton Trans.* **1988**, 2211−2213. (b) Deacon, G. B.; Forsyth, C. M.; Gatehouse, B. M.; Philosof, A.; Skelton, B. W.; White, A. H.; White, P. A. *Austr. J. Chem.* **1997**, *50*, 959−970.

(27) Holden, N. E. Table of the Isotopes. In *CRC Handbook of Chemistry and Physics*, 84th ed.; Lide, D. R., Eds.; CRC Press: Boca Raton, FL, 2004.

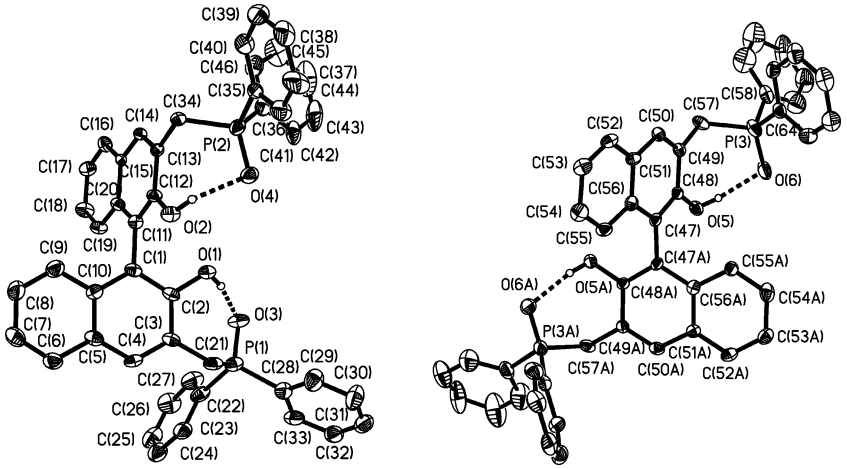

Figure 1. Molecular drawings of ligand precursor **1** showing 30% probability thermal ellipsoids. For ease of comparison, the two independent molecules are not shown in the actual mutual orientations. Hydrogen atoms (except those engaged in hydrogen-bonding) and disordered solvent molecules are omitted for clarity.

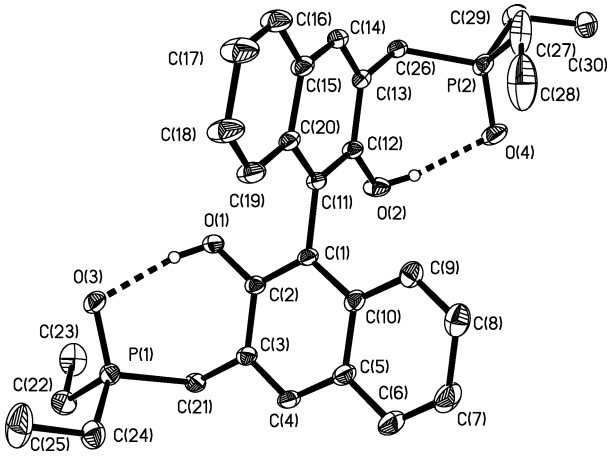

Figure 2. Molecular drawing of ligand precursor **2** showing 30% probability thermal ellipsoids. Hydrogen atoms (except those engaged in hydrogen-bonding) are omitted for clarity.

For example, a ^{31}P shift of δ −1.19 ppm is measured, from δ 43.82 ppm for the neutral ligand of **7** to δ 42.63 ppm after 1:1.1 reaction with La[N(SiMe$_3$)$_2$]$_3$, and a further shift to δ 42.10 ppm is observed after aminoalkene substrate introduction. The resonances both before and after substrate addition are broad, suggesting exchange between free and coordinated phosphine sulfide moieties. For reactions of these ligands with Nd[N(SiMe$_3$)$_2$]$_3$, which induces the largest ^{31}P shift in the presence of the phosphine oxide analogues, a broad ^{31}P resonance at 47.80 ppm (δ +3.98 ppm) appears in the Nd[N(SiMe$_3$)$_2$]$_3$ + ligand **7** (1:1.1 molar ratio) mixture after the addition of the substrate. The smaller shifts and broad signals suggest weak, labile binding between the phosphine sulfide moieties and the Ln^{3+} ions.

All efforts to obtain crystals of {(*R*)-BINOL-[P(O)R$_2$]$_2$}LnN(SiMe$_3$)$_2$ complexes suitable for diffraction studies were unsuccessful. In attempts to obtain {(*R*)-BINOL-[P(O)R$_2$]$_2$}Ln-R crystals, R = unconverted or converted aminoalkene substrate, after several hydroamination reactions were complete, the reaction mixtures were freeze−thaw−degassed and the volatiles vacuum-transferred from the NMR tubes. The powdery residues from these reactions were collected and dissolved in small amounts of toluene, and pentane was slowly diffused in at −40 °C. In one case, a few crystals of La$_2${(*R*)-BINOL-[P(O)Ph$_2$]$_2$}$_3$ (**8**) were obtained from a reaction that contained a 10 mol % excess of (*R*)-H$_2$BINOL-[P(O)Ph$_2$]$_2$. The identity of this complex was further confirmed by independent synthesis from La[N(SiMe$_2$)$_3$] and excess (*R*)-H$_2$BINOL-[P(O)Ph$_2$]$_2$. The NMR spectra are distinctly different from those of {(*R*)-BINOL-[P(O)Ph$_2$]$_2$}LaN(SiMe$_3$)$_2$ and the other {(*R*)-BINOL-[P(O)Ph$_2$]$_2$}LnN(SiMe$_3$)$_2$ complexes. In the structure refinement for complex **8**, the SQUEEZE program was used to deal with severely disordered toluene and pentane molecules within the unit cell. A sketch of the molecule is shown below, and a molecular drawing and selected bond lengths and angles are shown in Figure 6 and Table 3, respectively.

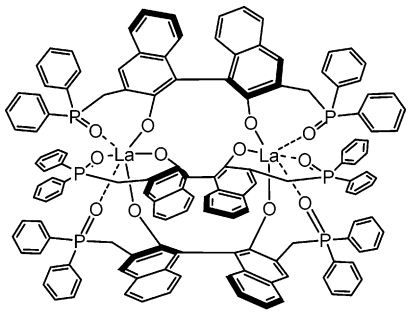

8

It can be seen that product **8** is a binuclear complex of composition La$_2${(*R*)-BINOL-[P(O)Ph$_2$]$_2$}$_3$. Three binaphtholate ligands span and chelate both La^{3+} ions in a propeller-like fashion. Both La^{3+} atoms are six-coordinate with three formally La−O two-center two-electron covalent bonds and three dative La←O bonds, and with a La−La distance of 4.802(3)Å. The formally two-center two-electron covalent bonds are from binaphtholate groups, while the dative ones are from phosphine oxide moieties. A distorted octahedral configuration is adopted around each La^{3+} ion, with a covalent bond *trans* to each dative one and with O−La−O angles of about 160° (Table 3). All covalent or dative bonds are almost mutually perpendicular (∠O−La−O = 76.1−107.5°). The formally two-center two-electron La−O covalent bond lengths range from 2.273(5) [La(2)−O(6)] to 2.299(6) Å [La(1)−O(5)], while the dative bond lengths lie between 2.469(5) [La(1)−O(11)] and 2.507(5) Å [La(1)−O(5)], consistent with similar lanthanum−oxygen bonding reported in the literature.[28]

Enantioselective Aminoalkene Hydroamination/Cyclization. Most of the present lanthanide binaphtholate complexes except those of diethoxy phosphine oxide moieties (**6**) display

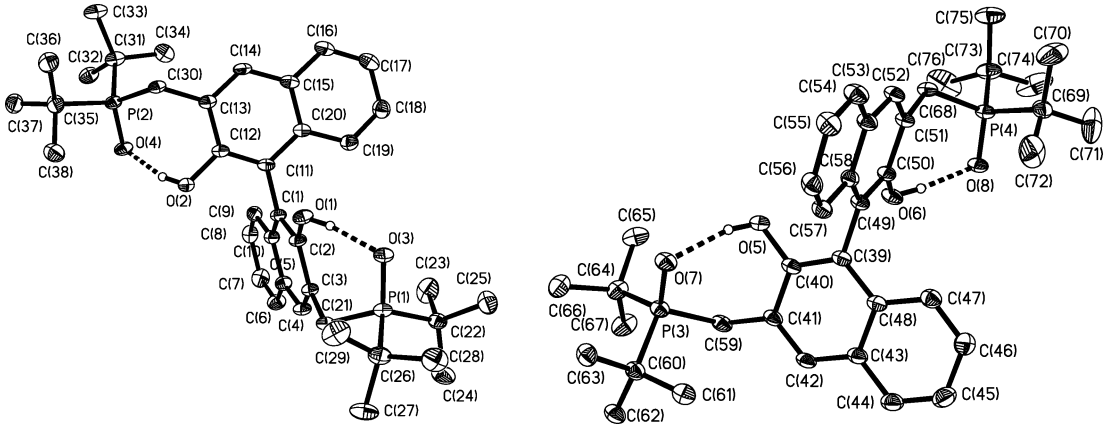

Figure 3. Molecular drawings of **3** showing 30% probability thermal ellipsoids. For ease of comparison, the two independent molecules are not shown in the actual mutual orientations. Hydrogen atoms (except those engaged in hydrogen-bonding) and toluene molecules are omitted for clarity.

Table 2. Selected Bond Distances (Å) and Angles (deg) for Ligand Precursors 1, 2, and 3

		1	
P(1)−O(3)	1.494(4)	P(2)−O(4)	1.490(4)
P(3)−O(6)	1.478(5)	P(4)−O(8)	1.506(5)
O(1)−C(2)	1.354(7)	O(2)−C(12)	1.365(6)
O(5)−C(48)	1.353(6)	O(7)−C(71)	1.363(7)
O(1)···O(2)	3.170	O(1)···O(3)	2.634
O(2)···O(4)	2.623	O(5)···O(5A)	3.865
O(3)···O(4)	6.256	O(6)···O(6A)	9.175
O(5)···O(6)	2.627		
O(3)−P(1)−C(21)	109.6(3)	O(4)−P(2)−C(34)	112.5(3)
O(6)−P(3)−C(57)	110.8(3)	O(8)−P(4)−C(80)	109.6(3)
P(1)−C(21)−C(3)	114.6(4)	P(2)−C(34)−C(13)	114.7(4)
P(3)−C(57)−C(49)	116.8(4)	P(4)−C(80)−C(72)	113.4(4)
		2	
P(1)−O(3)	1.503(2)	P(2)−O(4)	1.491(3)
O(1)−C(2)	1.368(4)	O(2)−C(12)	1.373(3)
O(1)···O(2)	3.624	O(1)···O(3)	2.677
O(3)···O(4)	8.983	O(2)···O(4)	2.714
O(3)−P(1)−C(21)	110.41(14)	O(4)−P(2)−C(26)	109.79(15)
P(1)−C(21)−C(3)	114.53(19)	P(2)−C(26)−C(13)	112.1(2)
		3	
P(1)−O(3)	1.511(2)	P(2)−O(4)	1.514(2)
P(3)−O(7)	1.510(2)	P(4)−O(8)	1.507(2)
O(1)−C(2)	1.354(4)	O(2)−C(12)	1.373(4)
O(5)−C(40)	1.370(4)	O(6)−C(50)	1.355(4)
O(1)···O(2)	3.783	O(1)···O(3)	2.612
O(3)···O(4)	9.010	O(2)···O(4)	2.666
O(5)···O(6)	3.651	O(5)···O(7)	2.659
O(6)···O(8)	2.629	O(7)···O(8)	8.904
O(3)−P(1)−C(21)	111.18(14)	O(4)−P(2)−C(30)	111.48(13)
O(7)−P(3)−C(59)	110.74(14)	O(8)−P(4)−C(68)	110.74(14)
P(1)−C(21)−C(3)	120.5(2)	P(2)−C(30)−C(13)	116.8(2)
P(3)−C(59)−C(41)	117.9(2)	P(4)−C(68)−C(51)	119.9(2)

catalytic activity at temperatures between 23 and 120 °C for the hydroamination/cyclization of **9** → **9a**. To find the catalytically optimal lanthanide ion and binaphtholate ligand combinations, the standard hydroamination was performed using the {(*R*)-BINOL-[P(O)R_2]$_2$}LnN(SiMe_3)$_2$ complexes generated in situ from NMR-scale reactions of 5 mol % Ln[N(SiMe_3)$_2$]$_3$ with 5.5 mol % of the corresponding binaphthol ligand precursor in benzene-d_6 (Table 4).

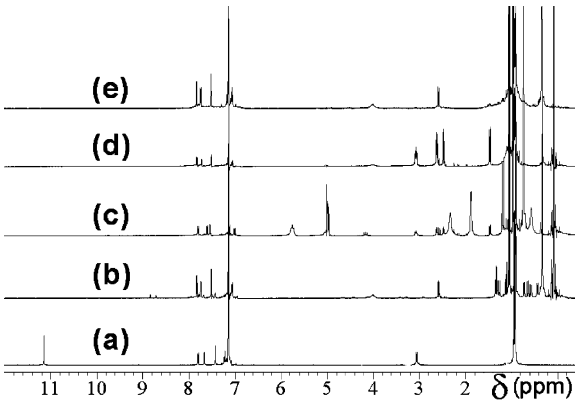

Figure 4. ^{1}H NMR step-plot of catalytic hydroamination of aminoalkene **9** by {(*R*)-BINOL-[P(O)^{t}Bu$_2$]$_2$}LuN(SiMe_3)$_2$ in benzene-d_6: (a) free ligand (*R*)-H_2BINOL-[P(O)^{t}Bu$_2$]$_2$; (b) precatalyst preparation in situ; (c) addition of substrate **9**; (d) completion of hydroamination; and (e) reaction mixture after removal of amines.

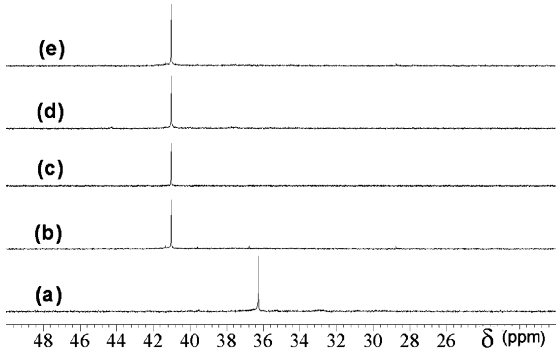

Figure 5. ^{31}P NMR step-plot of catalytic hydroamination of aminoalkene **9** by {(*R*)-BINOL-[P(O)Ph$_2$]$_2$}LaN(SiMe_3)$_2$ in benzene-d_6: (a) free ligand (*R*)-H_2BINOL-[P(O)Ph$_2$]$_2$; (b) precatalyst preparation in situ; (c) addition of substrate **9**; (d) completion of hydroamination; and (e) reaction mixture after removal of amines.

Lanthanide complexes with ligands **1** and **4** were investigated first, and it was found that ligand **1** complexes exhibit greater enantioselectivities than those of ligand **4**. The results then prompted us to investigate binaphtholate ligands with less sterically demanding organophosphine oxide substituents, prompting the synthesis of ligands **2**, **3**, and **5**, with anticipation that reduced steric encumbrance about the phosphine oxide would promote greater enantioselectivity. Efforts to prepare an even smaller methyl phosphine analogue of **2** resulted largely in

(28) (a) Cai, C.-X.; Amgoune, A.; Lehmann, C. W.; Carpentier, J.-F. *Chem. Commun.* **2004**, 330−331. (b) Nemoto, T.; Ohshima, T.; Yamaguchi, K.; Shibasaki, M. *J. Am. Chem. Soc.* **2001**, *123*, 2725−2732. (c) Butcher, R. J.; Clark, D. L.; Grumbine, S. K.; Vincent-Hollis, R. L.; Scott, B. L.; Watkin, J. G. *Inorg. Chem.* **1995**, *34*, 5468−5476. (d) Deacon, G. B.; Gatehouse, B. M.; Shen, Q.; Ward, G. N.; Thiekink, E. R. T. *Polyhedron* **1993**, *12*, 1289−1294. (e) Schaverien, C. J.; Meijboom, N.; Orpen, A. G. *J. Chem. Soc., Chem. Commun.* **1992**, 124−126.

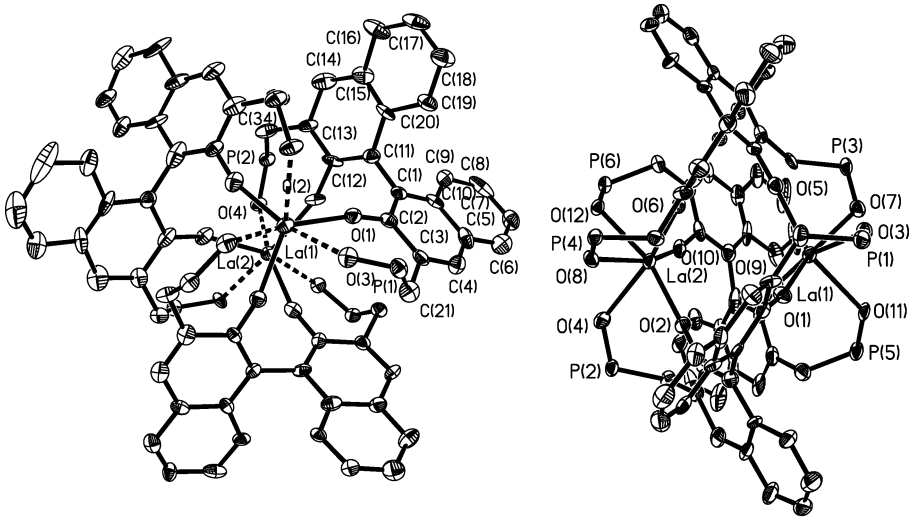

(a) **(b)**

Figure 6. Molecular drawings of complex **8** showing 30% probability thermal ellipsoids with two different viewing angles. Hydrogen atoms and phenyl groups in the bound phosphine oxide ligands are omitted for clarity.

Table 3. Selected Bond Distances (Å) and Angles (deg) for Complex 8

La(1)−O(1)	2.292(6)	La(1)−O(3)	2.494(6)
La(1)−O(5)	2.299(6)	La(1)−O(7)	2.489(6)
La(1)−O(9)	2.283(6)	La(1)−O(11)	2.469(5)
La(2)−O(2)	2.297(6)	La(2)−O(4)	2.474(6)
La(2)−O(6)	2.273(5)	La(2)−O(8)	2.473(5)
La(2)−O(10)	2.281(6)	La(2)−O(12)	2.507(5)
P(1)−O(3)	1.480(6)	P(2)−O(4)	1.508(6)
La(1)···La(2)	4.802		
O(1)−La(1)−O(7)	160.5(2)	O(3)−La(1)−O(9)	166.05(19)
O(5)−La(1)−O(11)	157.38(19)	O(1)−La(1)−O(3)	76.60(19)
O(1)−La(1)−O(5)	107.5(2)	O(1)−La(1)−O(9)	104.0(2)
O(1)−La(1)−O(11)	94.5(2)	O(2)−La(2)−O(12)	164.83(18)
O(4)−La(2)−O(6)	162.89(18)	O(8)−La(2)−O(10)	158.93(19)
O(2)−La(2)−O(4)	77.74(19)	O(2)−La(2)−O(6)	101.87(19)
O(2)−La(2)−O(8)	92.06(19)	O(2)−La(2)−O(10)	107.4(2)

Scheme 5. Simplified Catalytic Cycle for the Organolanthanide-Mediated Aminoalkene Hydroamination/Cyclization

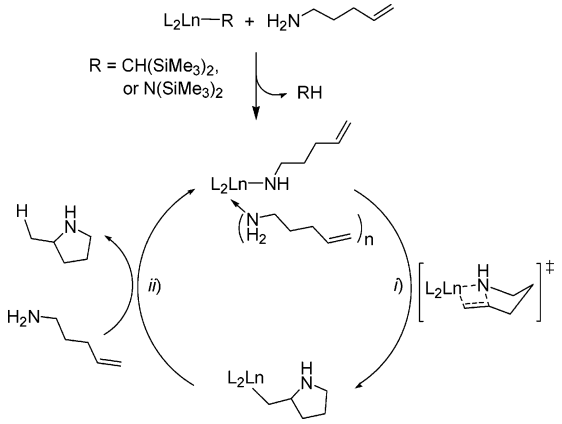

decomposition products. When complexes of ligand **2** were determined to exhibit the greatest enantioselectivity (entry 11) in this study, ethoxy ligand **6**, with differing neucleophilicity,[29] was prepared. However the lanthanide complexes of ligand **6** do not display significant hydroamination/cyclization activity. Phosphine sulfide ligand **7** was not investigated further after initial trials revealed poor enantioselectivity (entries 36 and 37 in Table 4). The poor selectivity with ligand **7** may reflect the weak binding of phosphine sulfide moieties to Ln^{3+} ions.

No detectable hydroamination activity is observed for complexes of ligand **6**, even at 120 °C, nor when using the homoleptic hydrocarbyl precursors ($Ln[CH(SiMe_3)_2]_3$, Ln = Y and Lu). This may reflect an increase in the effective electronegativity of the phosphine oxide moieties.[29] The Ln^{3+} Lewis acidity of the precatalysts is then plausibly strengthened, perhaps leading to stronger coordination of aminoalkene substrate molecules[3v] and thereby hindering the olefin insertion step in the hydroamination/cyclization cycle. All of the present catalytic systems effect quantitative **9** → **9a** conversion, judging from ^{1}H NMR spectra, except for some of the Sc^{3+} complexes: entry 23 (53% completion) and entry 17 (33%). No activity was detected for the Sc^{3+} complex of **4**. Generally, complexes with ligand **3** exhibit the highest turnover frequencies (entries 18−23).

Lanthanide ion size effects on enantioselectivity were investigated and were found to also depend on ligand architecture, as shown in Figure 7. For complexes of moderately encumbered ligand **1**, enantioselectivity increases slightly with decreasing Ln^{3+} ionic radius. However, the smallest Sc^{3+} ion affords the azacyclic product with an opposite stereochemical configuration and with ee = 58% (entry 8). In contrast, ee decreases with decreasing Ln^{3+} ionic radius for complexes of less encumbered ligand **2**, while again there is an inversion of product configuration for Sc^{3+}. The origin of this inversion for the Sc^{3+} catalysts with ligands **1** and **2** is not clear, and patterns of ^{1}H and ^{31}P NMR are observed during the hydroamination/cyclization process that are similar to the other lanthanide catalysts. Smaller selectivity variations with ionic radius are observed for ligands **2**, **3**, and **5**. Note that the Ln^{3+} complex of the most highly congested ligand, **4**, quantitatively yields an isomerization product, which has not been observed before in organolanthanide hydroamination/cyclization catalysis (eq 5) and suggests hindered access to the insertive HA transition state (Scheme 5).

(29) (a) Corbridge, D. E. C. In *Phosphorus* 2000, *Chemistry, Biochemistry & Technology*; Elsevier: Amsterdam, The Netherlands, 2000; pp 297−454. (b) Gilheany, D. G. Structure and Bonding in Phosphine Chalcogenides. In *The Chemistry of Organophosphorus Compounds*; Hartley, F. R., Eds.; John Wiley & Sons: West Sussex, England, 1990; Vol. 2.

Table 4. Catalytic Hydroamination/Cyclization Data for the Transformation 9 → 9a

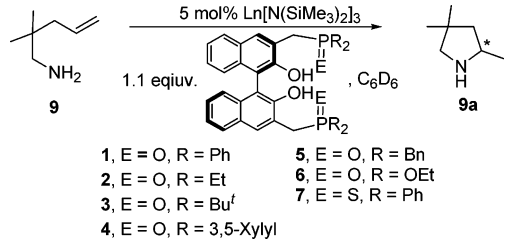

entry	precatalyst	T (°C)	N_t (h^{-1})	% ee (config.)
1	La-**1**	60	0.38	26 (*S*)
2	La-**1**	90	1.3	29 (*S*)
3	La-**1**	23	0.0056	20 (*S*)
4	Nd-**1**	60	0.69	27 (*S*)
5	Sm-**1**	60	0.26	40 (S)
6	Y-**1**	60	0.47	54 (*S*)
7	Lu-**1**	60	0.16	61 (*S*)
8	Sc-**1**	120	0.28	58 (*R*)
9	La-**2**	23	0.057	55 (*S*)
10	La-**2**	60	2.0	61 (*S*)
11	Nd-**2**	23	0.053	65 (*S*)
12	Nd-**2**	60	1.4	61 (*S*)
13	Sm-**2**	23	0.043	63 (*S*)
14	Sm-**2**	60	0.57	55 (*S*)
15	Y-**2**	60	0.25	9.6 (*S*)
16	Lu-**2**	60	0.067	7.5 (*S*)
17	Sc-**2**	120	0.0099	47 (*R*)
18	La-**3**	23	0.31	23 (*S*)
19	Nd-**3**	23	3.0	37 (*S*)
20	Sm-**3**	23	4.2	36 (*S*)
21	Y-**3**	23	20	32 (*S*)
22	Lu-**3**	23	1.2	37 (*S*)
23	Sc-**3**	120	0.26	1.7 (*S*)
24	La-**4**	60	0.96	isomerization
25	Nd-**4**	60	3.1	23 (*S*)
26	Sm-**4**	60	3.9	25 (*S*)
27	Y-**4**	60	2.8	42 (*S*)
28	Lu-**4**	60	0.49	26 (*S*)
29	Sc-**4**	120	N.R.	N.A.
30	La-**5**	23	0.16	40 (*S*)
31	Nd-**5**	23	0.23	32 (*S*)
32	Sm-**5**	23	0.14	13 (*S*)
33	Y-**5**	60	0.24	39 (*S*)
34	Lu-**5**	60	0.072	27 (*S*)
35	Sc-**5**	120	0.018	7.9 (*S*)
36	Sm-**7**	60	0.26	0.80 (*R*)
37	Y-**7**	60	0.82	7.4 (*S*)

Partial isomerizations of this type have been reported for Li[30a] and Pd[30b] HA catalysts.

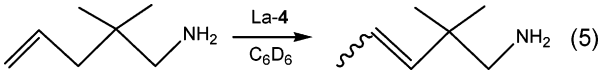

(5)

Reaction temperature effects on enantioselectivity are not as profound as those of ionic radius, as shown in Table 4. Enantioselectivity increases slightly as temperature is increased in some cases, whereas in other cases it declines modestly. Complex La-**1** exhibits the greatest selectivity drop from 29% ee at 90 °C to 20% at 23 °C.

Reaction Scope for {(*R*)-BINOL-[P(O)R$_2$]$_2$}LnN(SiMe$_3$)$_2$ Catalysts. Other aminoalkene substrates were also investigated for hydroamination/cyclization activity in forming five- and six-membered heterocycles (Table 5). Similar to C_1-symmetric chiral lanthanocene precatalysts,[31l–w] binaphtholate catalysts exhibit markedly substrate-specific reaction rates and enantioselectivities. Compared to the hydroamination of **9** → **9a**, the highest enantioselectivity for the conversion **10** → **10a** is only 26% ee, mediated by the catalyst Y-**1** (entry 4). Geminal diphenyl substitutions in the substrate carbon backbone accelerate turnover significantly, due to the Thorpe–Ingold effect[31] (entries 1–5). Unsubstituted substrate **11** can be cyclized only by complexes of ligand **3**, which exhibit the highest activity for **9** → **9a**.

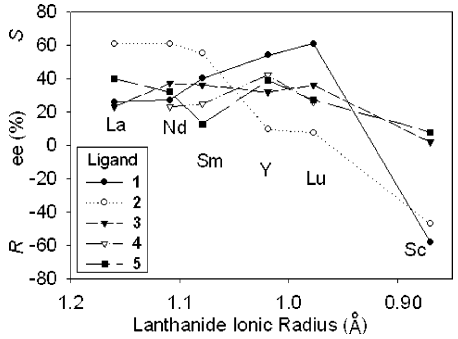

Figure 7. Plot of ee patterns for the **9** → **9a** transformation vs eight-coordinate lanthanide ionic radius for different {(*R*)-BINOL-[P(O)R$_2$]$_2$}$^{2-}$ catalyst ligand substitution.

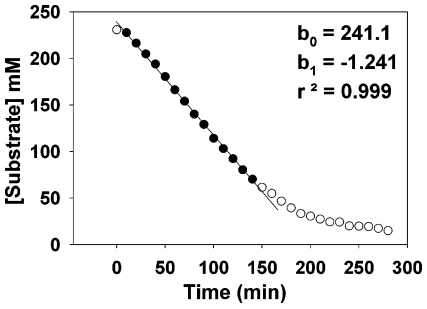

Figure 8. Substrate concentration as a function of time for the hydroamination/cyclization of **9** in benzene-d_6 at 23 °C mediated by catalyst of Y-**3**.

Table 5. Catalytic Hydroamination Results for Substrates 10–12

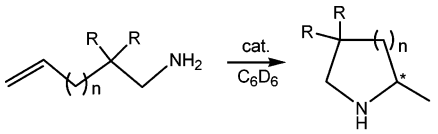

entry	precatalyst	substrate	T (°C)	N_t (h^{-1})	yield (%)	% ee (config.)
1	La-**1**	**10**	23	1.6	98	16 (*S*)
2	Nd-**1**	**10**	23	5.2	98	18 (*S*)
3	Sm-**1**	**10**	23	3.1	98	21 (*S*)
4	Y-**1**	**10**	60	2.1	98	26 (S)
5	Sc-**1**	**10**	120	0.16	60	11 (S)
6	Y-**7**	**10**	60	15	98	3.8 (*S*)
7	Y-**3**	**11**	60	0.071	40	23 (*S*)
8	Lu-**3**	**11**	60	0.074	30	24 (*S*)
9	La-**1**	**12**	120	0.049	56	1.5 (*S*)
10	Y-**1**	**12**	120	0.039	25	13 (*S*)
11	La-**2**	**12**	120	2.3	98	5.4 (*S*)
12	Nd-**2**	**12**	60	0.13	98	3.1 (*R*)
13	Y-**2**	**12**	120	0.053	98	4.7 (*S*)

(30) (a) Ates, A.; Quinet, C. *Eur. J. Org. Chem.* **2003**, 1623–1626. (b) Pugin, B.; Venanzi, L. M. *J. Am. Chem. Soc.* **1983**, *105*, 6877–6881.

(31) (a) Eliel, E. L.; Wilen, S. H. In *Stereochemistry of Organic Compounds*; John Wiley & Sons: New York, 1994; pp 682–684. (b) Kirby, A. J. *Adv. Phys. Org. Chem.* **1980**, *17*, 183–278.

A kinetic study of cyclization **9** → **9a** was carried out with the Y-**3** catalyst system by in situ ^{1}H NMR spectroscopy, as shown in Figure 8. The reaction rate is found to be zero-order in substrate over ~75.0% conversion, consistent with turnover-limiting intramolecular C═C insertion.[2b,3] Some departure from linearity is observed near complete conversion, and previous studies with other catalysts suggest that the substrate or product binding interferes with the turnover-limiting insertion step.[2b,3]

Conclusions

New chiral organophosphine oxide-substituted binaphtholate ligands were prepared and shown to have conformational flexibility and strong binding for lanthanide ions. Lanthanide complexes generated in situ from $Ln[N(SiMe_3)_2]_3$ reagents and the neutral binaphthol ligands cleanly catalyze enantioselective intramolecular hydroamination/cyclization of aminoalkenes with modest to good enantioselectivities at 23−120 °C. Kinetic studies indicate that the rate is zero-order in the concentration of amine substrate, suggesting the same mechanism as seen in previous organolanthanide-catalyzed hydroamination/cyclizations.

Acknowledgment. We thank NSF (Grant CHE-0078998) for support of this research and Dr. Bryan Stubbert, Holming Yuen, and Jiuqing Zhao for helpful discussions. We thank Ms. Charlotte L. Stern for the X-ray crystallographic data collection.

Supporting Information Available: X-ray crystallographic data, in CIF format, for **1**, **2**, **3**, and **8**. This material is available free of charge via the Internet at http://pubs.acs.org.

OM0607999